Scripta Materialia 208 (2022) 114336

Contents lists available at ScienceDirect

Scripta Materialia

journal homepage: www.elsevier.com/locate/scriptamat

Entropy-driven melting point depression in fcc HEAs

Tanner Kirk[b], Brent Vela[b], Seth Mehalic[b], Khaled Youssef[d], Raymundo Arróyave[a,b,c,*]

[a] Department of Materials Science and Engineering, Texas A&M University, College Station, TX 77843, USA
[b] Department of Mechanical Engineering, Texas A&M University, College Station, TX 77843, USA
[c] Department of Industrial and Systems Engineering, Texas A&M University, College Station, TX 77843, USA
[d] Qatar University – Physics Department, Materials Science and Technology Graduate Program, Doha, Qatar

ARTICLE INFO

Article history:
Received 1 July 2021
Revised 12 September 2021
Accepted 7 October 2021
Available online 16 October 2021

Keywords:
High entropy alloys
Alloy design
High temperature applications
Melting

ABSTRACT

High Entropy Alloys (HEAs) are an increasingly dominant alloy design paradigm. The premise of entropic stabilization of single-phase alloys has motivated much of the research on HEAs. Chemical complexity may indeed help stabilize single alloy phases relative to other lower-entropy competing solid phases. Paradoxically, this complexity may de-stabilize these alloys against the liquid phase, potentially limiting the application space of HEAs at elevated temperatures. In this work, we carry out a comprehensive investigation of the phase stability in the fcc CoCrFeMnNiV-Al HEA space using a state of the art CALPHAD database. By using modern visualization techniques and statistical analysis we examine the trade-off between chemical complexity and stability against the liquid state and identify a potentially difficult to overcome barrier for development of high temperature alloys, at least within the conventional fcc HEA space. Limited experimental data seem to be consistent with this analysis.

High Entropy Alloys (HEAs) are a dominant paradigm in alloy design seeking to exploit chemical complexity in order to overcome challenging performance trade-offs that otherwise would be very difficult to resolve using conventional alloys at the corners/edges of the composition space [1–3]. Out of the thousands of HEAs investigated thus far, most of them perform at best as well as conventional alloys. It must be pointed out, however, that there have been a number of alloys tat certainly belong to the performance Pareto front in the alloy space with improved ductility [4,5], fatigue strength [6,7], fracture toughness [8], and thermal stability relative to their conventional counterparts.

The "high entropy" adjective was initially used as the distinctive qualifier for this alloy paradigm as the existence of stable wide single-phase solid solutions within the composition space was ascribed to increased configurational entropy. Phase stability, however, is not exclusively a consequence of competition among phases through entropy [1]. One could use entropy arguments to justify the stabilization of solid solutions relative to ordered competing phases with less configurational entropy. Analysis of some systems, however, suggests that differences in configurational entropies between ordered and disordered phases at temperatures close to the order-disorder transition are negligible [9]. In the case of phase competition among disordered phases (e.g. hcp vs. bcc), entropy should play an even less defining role, given that such phases are likely to have very similar configurational entropies [10].

Different solution phases in the solid state may thus not 'out-compete' each other significantly on configurational entropy grounds. In fact, there is recent evidence [10] that there are enthalpic effects associated to atomic distortions that play a non-trivial role in the stability of bcc HEAs in competition with their hcp forms. Yet, one aspect of the phase competition among similarly disordered phases that has not been explored systematically and that can have significant consequences for the search of high-perfomance alternatives to high-temperature structural materials such as Ni-based superalloys is the actual effect of compositional complexity on the melting point of a given alloy, as this constitutes the absolute limit of stability of a given material.

In this work, we focused on the CoCrFeMnNiV-Al fcc HEA space, as this alloy system has been suggested to be the basis for potential alternatives to Ni-based superalloys [11]. While alloys within this space have been shown to exhibit satisfactory mechanical performance it is worth looking into the stability of the fcc solid solution in this space against melting, from a global perspective. To this effect, we proceeded to exhaustively sample the phase stability of this alloy space using a CALPHAD approach with the TCHEA3 thermodynamic database [12]. We started with 10^6 uniform random samples of the total composition space, but focused our search on alloys with less than 10 at.% Al (467,228 alloys). We then calculated phase equilibria to identify alloys predicted to form 100% fcc

* Corresponding author at: Department of Materials Science and Engineering, Texas A&M University, RDMC 216, College Station, TX 77843, USA.
E-mail address: rarroyave@tamu.edu (R. Arróyave).

https://doi.org/10.1016/j.scriptamat.2021.114336
1359-6462/

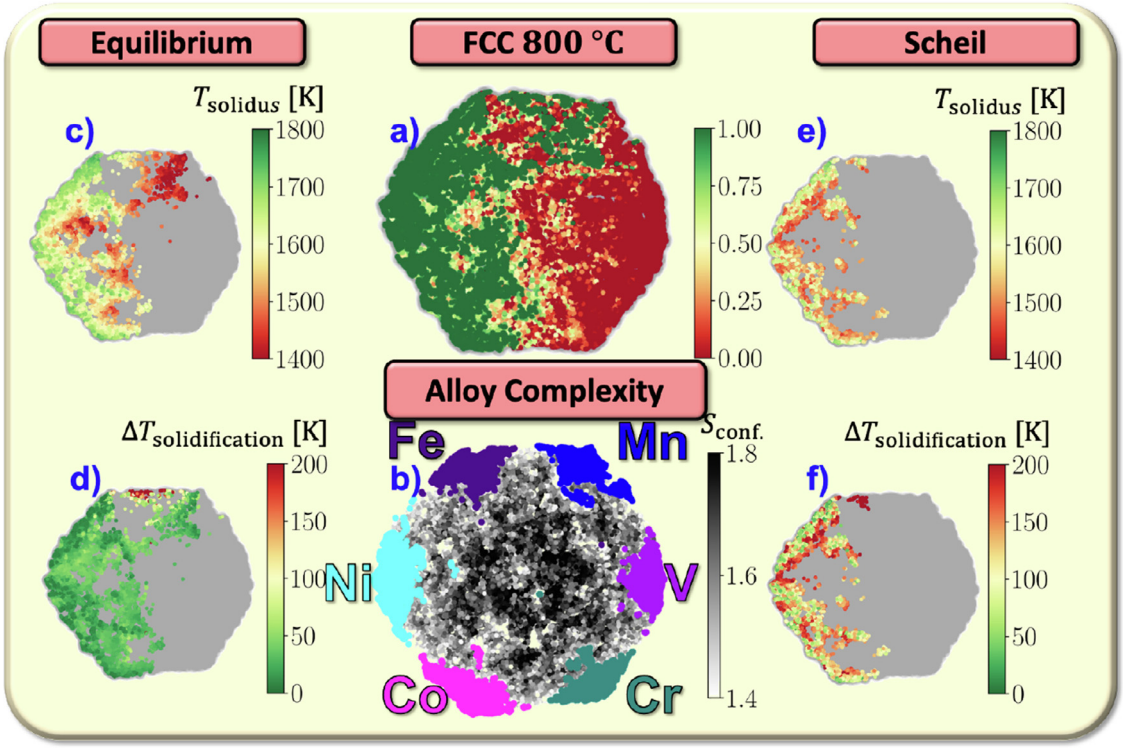

Fig. 1. 2-D projection using t-distributed stochastic neighbor embedding (t-SNE) of the phase stability space in the 7-dimensional CoCrFeMnNiV-Al fcc HEA space. *Note:* Except for (b), points where the plotted quantity was not calculated are shown in gray. a) Predicted phase fraction for fcc solid solution at 800 °C; b) Alloy complexity, measured as the *maximum* possible configurational entropy, $S_{conf.}$ of a given alloy; c) Predicted equilibrium solidus temperature for alloys that exist as fcc at 800 °C; d) Predicted equilibrium solidification range for alloys that exist as fcc at 800 °C; e) Predicted solidus temperature under Scheil solidification conditions (infinite diffusion in the liquid and no diffusion in the solid); f) Predicted solidification range under Scheil solidification conditions.

at 800 °C. Notably, only 36,294 alloys, less than 4% of the original alloy space, met both of these constraints. Given our interest in high-temperature applications we decided to further constrain the search space by conducting equilibrium solidification simulations and identifying alloys with a solidus temperature above 1600 K (i.e. higher than the melting range of Ni-based super alloys). Only 20,541 alloys or **2%** of the total HEA space explored met this further constraint. In addition to predicting the equilibrium competition between fcc and liquid, we also carried out Scheil simulations [13] (with a step size of 1 K) for the 2% of alloys predicted to be fcc and suitable for high temperature applications. Scheil simulations account for solute segregation in the remaining liquid upon solidification and are thus more conservative in their estimate of liquid phase stability-most solidification processes are far from equilibrium.

Fig. 1 summarizes the results of the analysis described above. Given the high-dimensional nature of the explored HEA space, we project it using t-distributed stochastic neighbor embedding (t-SNE). In this projection, alloys of similar composition are 'close' to each other although no quantitative estimate as to this distance can be made. The projection shows—see Fig. 1b)—alloys in which one constituent is the majority element belonging to one of the corners of the 'hexagon'—Al is not a major constituent in any of the alloys by design. Unsurprisingly, the analysis shows that fcc phase stability (Fig. 1a)) is associated with regions dominated by Fe, Ni, and Co. However, fcc stability is observed well within the t-SNE projection, in regions dominated by senary systems with $S_{conf.} \sim 1.8$ J/K as shown in Fig. 1b)—$S_{conf.}$ is used here only as an indicator of alloy complexity.

We then focused our attention on the competition between the solid and the liquid phases across this 7-dimensional alloy space. As mentioned above, only a very small fraction of this space contains alloys that could potentially compete with Ni-based superalloys—at least from the perspective of their melting temperature. By examining Fig. 1c) and e) we first notice that the high-melting-temperature region in the space is located close to the Fe/Ni/Cr edges of the space. Moreover, when one accounts for the non-equilibrium nature of solidification prevalent under most processing conditions we can see that the high-melting region is further reduced, as a consequence of the alloy solubility differences between the liquid and the solid phases. The effect of segregation on the solidification range of alloys in this system can be seen by comparing Fig. 1d) and f): when considering equilibrium solidification conditions, a large fraction of the feasible alloys (fcc at 800 °C and $T_m > 1600$ K) have a relatively narrow solidification range, which may be beneficial as it decreases the potential for microsegregation during solidification. Once segregation is accounted for, the solidification range tends to expand significantly.

Going back to the predicted trends in melting temperatures ($T_{solidus}$), one can observe that there is a definite gradient in the stability of the fcc solid solutions as the alloys move towards the center of the composition space. Fig. 1 shows that the central region of the t-SNE plot is associated with the highest alloy complexity (i.e. highest maximum potential configurational entropy). Using configurational entropic arguments, this region would correspond to a maximum stabilization of fcc solid solutions. We note, however, that this stabilization may take place, if at all, against phases expected to have lower configurational entropy, such as ordered or semi-ordered phases. In contrast, the analysis in Fig. 1 suggests that fcc solid solutions do not compete favorably with the disordered liquid phase. Without delving into details, one could expect that the configurational entropy in the solid state is in fact significantly less than what can be maximally attained—previous work [9] suggests that even for moderately interacting

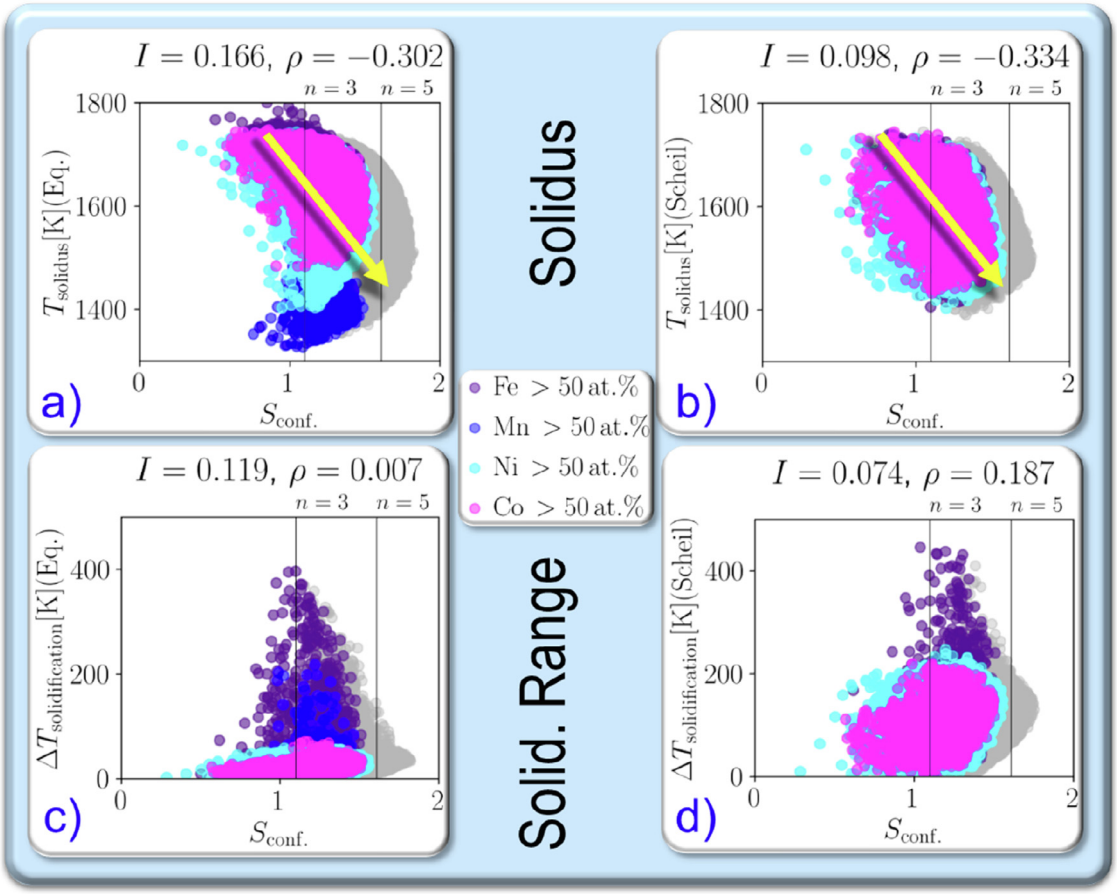

Fig. 2. Dependence of melting behavior on (maximum) configurational entropy for the CoCrFeMnNiV-Al fcc HEA system. Different colors correspond to alloys in which there is a component that exists at more than 50%, with gray corresponding to alloys without a majority constituent. Vertical lines denote the configurational entropy of ternary ($n = 3$) and a quinary ($n = 5$) alloys, respectively. I and ρ refer to mutual information and Pearson correlation coefficient, respectively.

multi-component systems ideality (i.e. perfect randomness) is only achievable at temperatures well above an alloy's melting point. On the other hand, while some degree of SRO could potentially be observed in the liquid, it is a reasonable assumption that the configurational entropy in the liquid state would be higher than in the solid state—the same can be stated of other entropic contributions.

A preliminary look at the impact of configurational entropy on the melting point of alloys in the CoCrFeMnNiV-Al fcc HEA system is shown in Fig. 2. In this figure, the solidification temperature as well as solidification range are grouped in terms of the majority element (or lack thereof). Fig. 2a) shows that there is a (admitedly somewhat weak) correlation between $T^{\text{eq.}}_{\text{solidus}}$ and $S_{\text{conf.}}$, in agreement with the notion that configurational entropy may place compositionally complex solid solution phases at a disadvantage with respect to an equally complex liquid phase. An exception to this negative correlation comes from fcc alloys that have excess Mn due to the relatively low melting point of the latter. In this case, the "averaging" effect resulting from alloying with constituents with higher melting points likely results in an overall increase in the solidus temperature, particularly with alloys with complexity equivalent to a ternary or higher. This correlation is even stronger when computing the solidus temperature under Scheil solidification conditions, as shown in Fig. 2b).

We have investigated the Pareto front of the highest $T^{\text{eq.}}_{\text{solidus}}$ and highest $S_{\text{conf.}}$ of Fig. 2a) and found that compositions with *maximum* entropy and *maximum* solidus temperature contain Ni, Fe, and Co in the highest concentrations relative to the entire alloy population. Moreover, these alloys are richer in Cr and leaner in Mn. Visualization of these insights is provided as supplementary material (see Fig. S1).

Another interesting trend that we have captured from this analysis is the relationship between $S_{\text{conf.}}$ and the solidification range, $\Delta T_{\text{sol.}}$ under both equilibrium and Scheil solidification conditions. Fig. 2c) and d) show that $\Delta T_{\text{sol.}}$ is narrower in the case of both low- and high-complexity alloys. The simplest alloys (those corresponding to a dilute solution with a single major solvent) are expected to have narrow solidification ranges, at least under equilibrium conditions. When accounting for solute partitioning under Scheil solidification conditions the solidification ranges widen, but the trend remains the same. In both cases, though, there seems to be a peak in the variance in solidification range that is located at a $S_{\text{conf.}}$ corresponding to a ternary alloy. As the alloy complexity increases, there is much less variance in the solidification range. This can be explained because the differences among quinary alloys are less pronounced than among ternaries. The fact that the solidification range is narrower as the composition complexity increases could in turn be explained by the fact that entropic effects in both the solid and liquid phases in these systems are the likely dominant contributors to phase stability. When enthalpic effects are not as important, the Gibbs energies of mixing tend to be similar in the liquid and solid phases, resulting in a narrow solidification range.

While Fig. 1 makes a (weak) case for the relationship between $S_{\text{conf.}}$ and the solidification range, $\Delta T_{\text{sol.}}$, it is necessary to ask whether a stronger connection could be justified. As a rough approximation, one could start with the well-known result for the

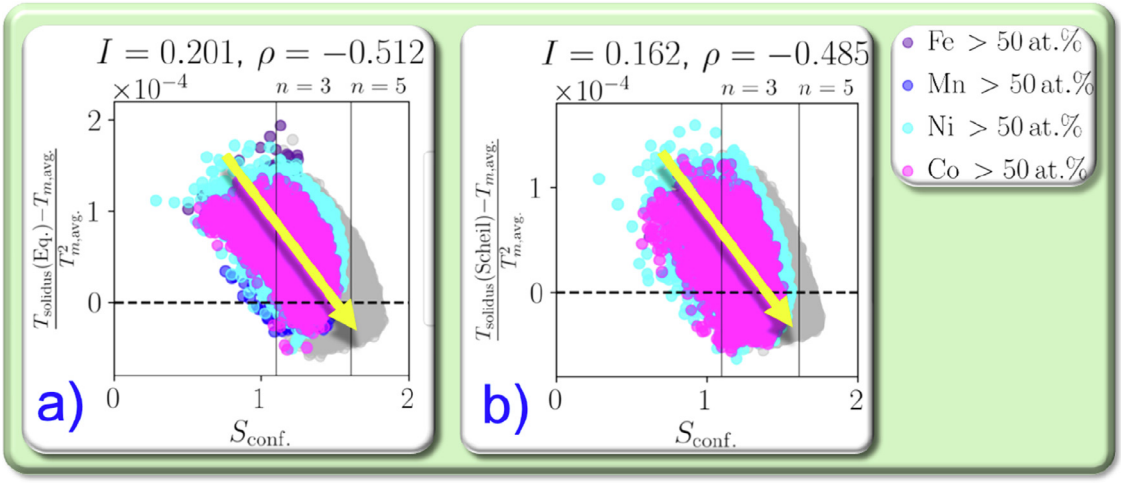

Fig. 3. Dependence of $\frac{T_{\text{solidus}} - T_{m,\text{avg}}}{T^2_{m,\text{avg}}}$ with $S_{\text{conf.}}$ for the CoCrFeMnNiV-Al fcc HEA system. This figure shows a strong negative correlation between the melting point of an alloy and the alloy complexity.

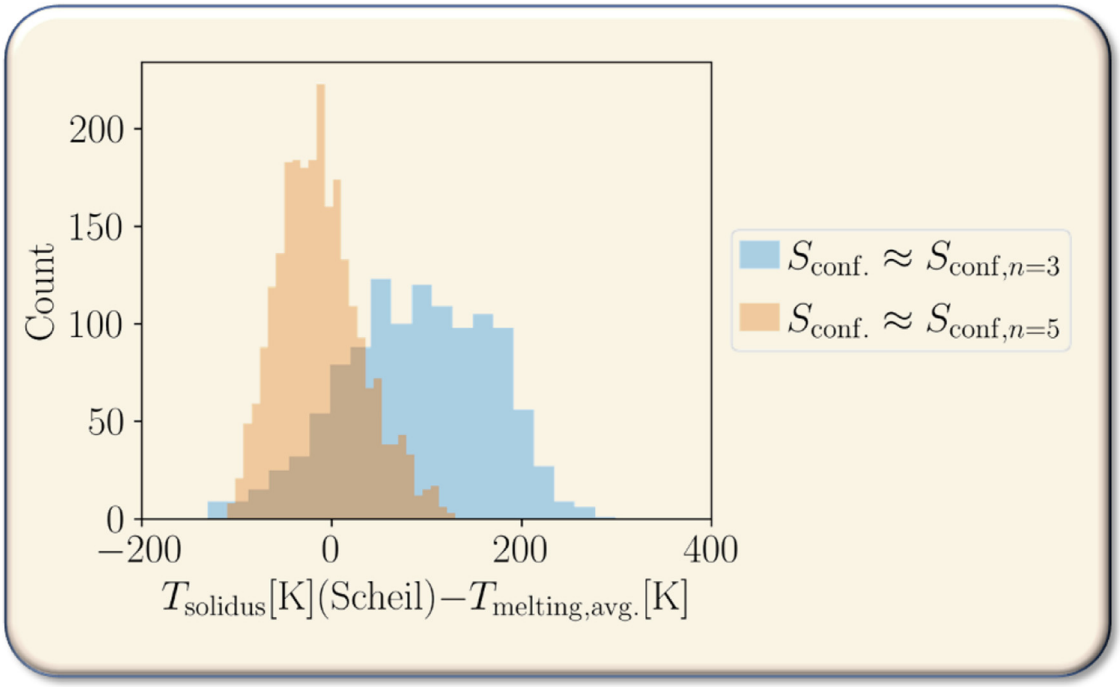

Fig. 4. Distribution of melting point depression, $T_{\text{solidus}} - T_{m,\text{avg}}$ for alloys with chemical complexity equivalent to that of a ternary vs. a quinary alloy.

melting point depression—note that this is not the solidification range—in a binary alloy as compared to a pure solvent:

$$\frac{\Delta T_m}{T_m^2} = \frac{T_{\text{solidus}} - T_{m,\text{avg}}}{T^2_{m,\text{avg}}} =\sim \frac{R \ln (x_A)}{\Delta H_{m,\text{fus}}} \tag{1}$$

where $\Delta H_{m,\text{fus}}$ corresponds to the latent heat of melting. Assuming that the latter is a weak function of temperature, the expression above suggests that, all things being equal, the melting point of an alloy should drop as its chemical complexity increases. Of course, the expression above may exaggerate the fact that the liquid is expected to have higher entropy, as the underlying assumption of the model above is that the solid phase does not have any configurational entropy.

A further complication is the fact that there remain averaging effects that need to be discarded in order to give strength to the entropic one. We thus decided to use Eq. (1), replacing T_m by the atomic fraction-weighed *average* melting point for a given alloy. By accounting for this 'averaging' effect it is possible to isolate entropic effects more effectively. In Fig. 3 we visualize Eq. (1) against the current fcc dataset. In this case, the correlation between the melting point depression and the configurational entropy is much stronger. The overall trend and the shape of the distribution in melting point depression considering either equilibrium or Scheil simulation conditions is remarkably similar, with a slight shift downward for the latter. In this case, for all systems (even the low-melting Mn-rich fcc alloys), a higher chemical complexity results in a lowering of the melting point of the alloy, relative to the averaged melting point. This seems to lend credence to the hypothesis motivating this work.

In Fig. 4 we show the distribution in the melting point depression for ternary- and quinary-like alloys within the larger CoCrFeMnNiV-Al fcc HEA space. The degree of complexity of the alloy was inferred from the maximum $S_{\text{conf.}}$ attainable. The figure shows that there is a statistically meaningful difference in the so-

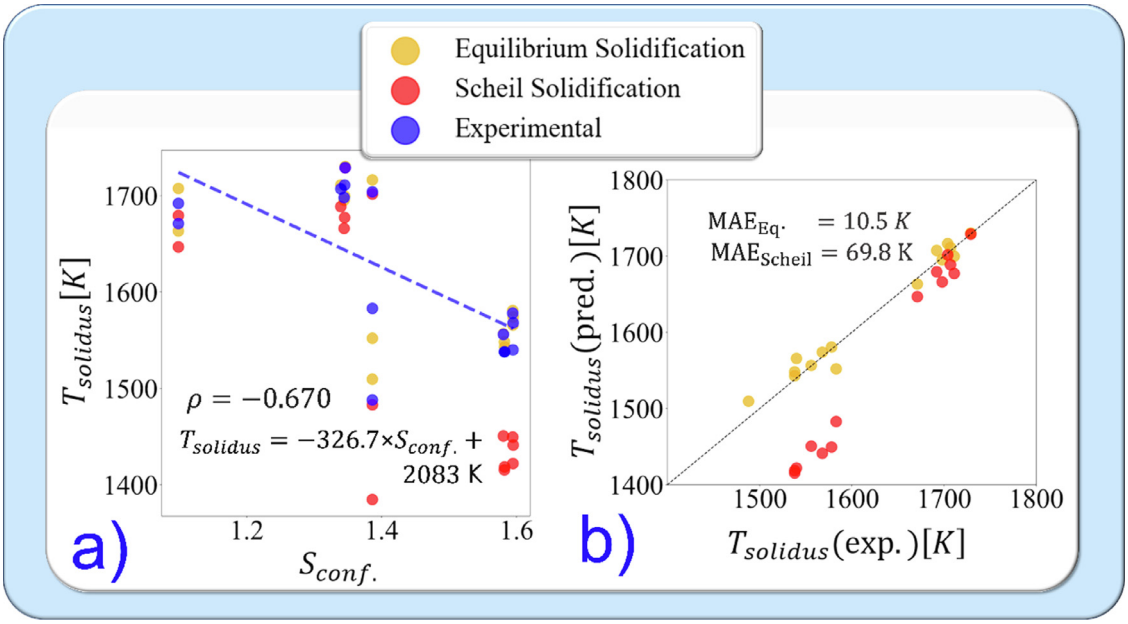

Fig. 5. a) Dependence of solidus temperature with (maximum possible) configurational entropy or chemical complexity; b) Parity plot comparing calculated and experimental solidus temperature. Solidus calculations are carried out considering both equilibrium and Scheil simulation conditions. ρ corresponds to the Pearson correlation between temperatures or temperature-related functions and (maximum possible) configurational entropy.

lidification behavior as a function of alloy complexity, with quinary alloys having lower melting points than their ternary counterparts. Interestingly, this analysis also suggests that in the case of low-order systems, the melting point is *actually higher* than what one could expect from averaging the melting point of the constituent elements. This 'over-stabilization' of the solid solution relative to the liquid phase likely originates from exothermic enthalpic effects. While it is likely that to a first approximation the constituents in the liquid interact in a qualitatively similar manner (i.e. through exothermic interactions), the shorter interatomic distances and more ordered nature of unlike bonds in the solid are likely to result in a phase-competitive advantage. While in low order systems these effects seem to overcome entropy, the switch from enthalpy-controlled to entropy-controlled melting seems to occur at $N = 3$, which is in line, incidentally, with an analysis carried out by Curtarolo's group [14] on entropic and enthalpic effects on phase competition in the solid state.

Having established the negative correlation between the calculated melting temperatures and the maximum possible configuration in the CoCrFeMnNiV-Al fcc HEA, we proceeded to find experimental validation for these predictions. The data of the solidification behavior of HEAs is sparse, but there are some recent works in which this has been studied [15–19]—we have added the raw data as a supplementary file. Fig. 5a) shows a negative correlation ($\rho - 0.67$) between experimental solidus temperature and alloy complexity, in agreement with our analysis based on CALPHAD-based simulations. *Experiments thus strongly suggest that configurational entropy does decrease the melting point of (fcc) HEAs.* Importantly, Fig. 5b) shows that when comparing experiments and observations, the agreement is excellent (MAE$\sim$ 10.5 K), provided we assume equilibrium solidification conditions. While sparse, this experimental evidence provides confidence in our computational analysis over the entire fcc HEA space under investigation.

To close, we have investigated whether configurational entropy, often put forward as a key factor in the stabilization of single phase solid solutions in the HEA space, has an effect on the melting point of fcc HEAs. Our analysis suggests that there is a negative correlation between alloy complexity—mapped to a (maximum) possible configurational entropy, S_{conf}—and melting point. This is also verified using a simple analysis of the thermodynamics of melting of solid solutions. *Notably, we have collected some experimental measurements that seem to align with our CALPHAD-based analysis: there is a trade-off between alloy complexity and melting.* These results suggest that although there may be valid reasons to want to explore the 'high entropy' region in the HEA space, alloy complexity comes at the price of lower melting points, which can be an important consideration when considering these fcc HEA alloys as potential replacements of Ni-based super alloys, for example.

Declaration of Competing Interest

The authors declare that they have no known competing financial interests or personal relationships that could have appeared to influence the work reported in this paper.

Acknowledgments

RA and KY acknowledge the support of QNRF under Project no. NPRP11S-1203-170056. TK and BV acknowledge the support of NSF through Grant no. NSF-DGE-1545403. RA, BV and SM acknowledge the support from ARPA-E ULTIMATE Program through Project DE-AR0001427. High-throughput CALPHAD calculations were carried out in part at the Texas A&M High-Performance Research Computing (HPRC) Facility.

Supplementary material

Supplementary material associated with this article can be found, in the online version, at doi:10.1016/j.scriptamat.2021.114336.

References

[1] D. Miracle, O. Senkov, Acta Mater. 122 (2017) 448–511.
[2] M.C. Gao, J.-W. Yeh, P.K. Liaw, Y. Zhang, High-Entropy Alloys: Fundamentals and Applications, Springer, 2016.
[3] E.P. George, W. Curtin, C.C. Tasan, Acta Mater. 188 (2020) 435–474.
[4] O. Senkov, S. Senkova, C. Woodward, Acta Mater. 68 (2014) 214–228.

[5] Z. Li, K.G. Pradeep, Y. Deng, D. Raabe, C.C. Tasan, et al., Nature 534 (2016) 227–230.
[6] M.A. Hemphill, T. Yuan, G. Wang, J. Yeh, C. Tsai, A. Chuang, P. Liaw, Acta Mater. 60 (2012) 5723–5734.
[7] Z. Tang, T. Yuan, C.-W. Tsai, J.-W. Yeh, C.D. Lundin, P.K. Liaw, Acta Mater. 99 (2015) 247–258.
[8] M. Seifi, D. Li, Z. Yong, P.K. Liaw, J.J. Lewandowski, JOM 67 (2015) 2288–2295.
[9] C.G. Schön, T. Duong, Y. Wang, R. Arróyave, Acta Mater. 148 (2018) 263–279.
[10] G. Samolyuk, Y. Osetsky, G. Stocks, J. Morris, Phys. Rev. Lett. 126 (2021) 025501.
[11] J. He, H. Wang, H. Huang, X. Xu, M. Chen, Y. Wu, X. Liu, T. Nieh, K. An, Z. Lu, Acta Mater. 102 (2016) 187–196.
[12] H. Mao, H.-L. Chen, Q. Chen, J. Phase Equilib. Diffus. 38 (2017) 353–368.
[13] E. Scheil, Z. Met. 34 (1942) 70–72.
[14] C. Toher, C. Oses, D. Hicks, S. Curtarolo, Npj Comput. Mater. 5 (2019) 1–3.
[15] A.F. Andreoli, O. Shuleshova, V.T. Witusiewicz, Y. Wu, Y. Yang, O. Ivashko, A.-C. Dippel, M.v. Zimmermann, K. Nielsch, I. Kaban, Acta Mater. 212 (2021) 116880.
[16] M. Bloomfield, K. Christofidou, N. Jones, Intermetallics 114 (2019) 106582.
[17] M. Bloomfield, K. Christofidou, F. Monni, Q. Yang, M. Hang, N. Jones, Intermetallics 131 (2021) 107108.
[18] K. Christofidou, T. McAuliffe, P. Mignanelli, H. Stone, N. Jones, J. Alloys Compd. 770 (2019) 285–293.
[19] A. Durand, L. Peng, G. Laplanche, J. Morris, E. George, G. Eggeler, Intermetallics 122 (2020) 106789.